Acta Crystallographica Section D
Biological Crystallography
ISSN 0907-4449

High-resolution crystal structure of an avidin-related protein: insight into high-affinity biotin binding and protein stability

Yael Eisenberg-Domovich,[a] Vesa P. Hytönen,[b] Meir Wilchek,[c] Edward A. Bayer,[c] Markku S. Kulomaa[b]‡ and Oded Livnah[a]*

[a]Department of Biological Chemistry, The Institute of Life Sciences, The Wolfson Centre for Applied Structural Biology, The Hebrew University of Jerusalem, Givat Ram, Jerusalem 91904, Israel, [b]NanoScience Center, Department of Biological and Environmental Science, FIN-40014 University of Jyväskylä, Finland, and [c]Department of Biological Chemistry, The Weizmann Institute of Science, 76100 Rehovot, Israel

‡ Current address: Institute of Medical Technology (IMT), Biokatu 6, FIN-33014, University of Tampere, Finland.

Correspondence e-mail: oded.livnah@huji.ac.il

© 2005 International Union of Crystallography
Printed in Denmark – all rights reserved

Received 9 November 2004
Accepted 3 February 2005

PDB References: baculovirus-expressed AVR4–biotin complex, 1y52, r1y52sf; bacterial-expressed AVR4, 1y53, r1y3sf; bacterial-expressed AVR4–biotin complex, 1y55, r1y55sf.

The chicken avidin gene belongs to an extended gene family encoding seven avidin-related genes (*AVR*s), of which only avidin is expressed in the chicken. The sequences of AVR4 and AVR5 are identical and the common protein (AVR4) has been expressed both in insect and bacterial systems. The recombinant proteins are similarly hyperthermostable and bind biotin with similarly high affinities. AVR4 was crystallized in the apo and biotin-complexed forms and their structures were determined at high resolution. Its tertiary and quaternary structures are very similar to those of avidin and streptavidin. Its biotin-binding site shows only a few alterations compared with those of avidin and streptavidin, which account for the observed differences in binding affinities. The increased hyperthermostability can be attributed to the conformation of the critical L3,4 loop and the extensive network of 1–3 inter-monomeric interactions. The loop contains a tandem Pro-Gly sequence and an Asp-Arg ion pair that collectively induce rigidity, thus maintaining its closed and ordered conformation in both the apo and biotin-complexed forms. In addition, Tyr115 is present on the AVR4 1–3 monomer–monomer interface, which is absent in avidin and streptavidin. The interface tyrosine generates inter-monomeric interactions, *i.e.* a tyrosine–tyrosine π–π interaction and a hydrogen bond with Lys92. The resultant network of interactions confers a larger 1–3 dimer–dimer contact surface on AVR4, which correlates nicely with its higher thermostability compared with avidin and streptavidin. Several of the proposed thermostability-determining factors were found to play a role in strengthening the tertiary and quaternary integrity of AVR4.

1. Introduction

Chicken egg-white avidin and its bacterial analogue streptavidin are homotetrameric proteins that share extremely high affinities towards the vitamin D-biotin (Green, 1975, 1990). The tetrameric structure of the proteins is essential for their high affinity for biotin. The high affinity between these proteins and biotin has been extensively exploited as a powerful and indispensable tool in many biotechnological and biomedical applications (Bayer & Wilchek, 1990; Wilchek & Bayer, 1990).

Avidin and streptavidin share approximately 30% identity and 40% similarity in their primary structures and consequently their tertiary fold and quaternary arrangement are highly similar. The tertiary fold of avidin and streptavidin consists of an eight-stranded antiparallel β-barrel; the main difference between the two proteins lies in the size, composition and conformation of the loops connecting the strands

(Hendrickson *et al.*, 1989; Weber *et al.*, 1989; Livnah *et al.*, 1993).

Avidin and streptavidin tetramers contain four biotin-binding sites, one per each monomer, with a highly similar arrangement of amino-acid residues within the respective binding pockets (Hendrickson *et al.*, 1989; Weber *et al.*, 1989; Livnah *et al.*, 1993). A critical tryptophan residue (Trp110 and Trp120 in avidin and streptavidin, respectively) is contributed to the biotin-binding site from a neighbouring monomer and plays an essential role in both biotin binding and oligomeric stability (Sano *et al.*, 1997; Freitag *et al.*, 1998; Laitinen *et al.*, 1999).

In the apo forms of avidin and streptavidin, the loop connecting strands $\beta3$ and $\beta4$ (L3,4) is disordered (Livnah *et al.*, 1993; Freitag *et al.*, 1997). Upon binding biotin, the L3,4 loop becomes ordered and forms hydrogen-bonding interactions with the ligand in a lid-like arrangement (Korndorfer & Skerra, 2002; Pazy *et al.*, 2003). In avidin, the L3,4 loop is three residues larger than in streptavidin and shows higher flexibility (Pazy *et al.*, 2002).

The quaternary arrangement of the two proteins consists of four identical subunits, each monomer in which exhibits three types of interactions with its adjacent subunits (Hendrickson *et al.*, 1989; Weber *et al.*, 1989; Livnah *et al.*, 1993). Subunits 1 and 4 (numbered according to Livnah *et al.*, 1993) share the largest contact area, with numerous accompanying intermolecular interactions. The contact area between the two 1–4 dimers consists of the 1–2 and 1–3 monomer–monomer interactions combined. Despite the similarities, the two proteins differ in many of their molecular properties. For example, streptavidin is a neutral nonglycosylated protein, as opposed to avidin, which is glycosylated and positively charged (pI $\simeq$ 10.5). In addition, because of the differences in their respective molecular surfaces, the two proteins lack immunochemical cross-reactivity. Avidin and streptavidin share high thermal stability, which further increases after the biotin complex is formed. The observed transition midpoint of heat denaturation (T_m) for avidin is even higher than that of streptavidin (Gonzalez *et al.*, 1999; Waner *et al.*, 2004).

The chicken avidin gene (*AVD*) belongs to an extended gene family that encodes seven avidin-related genes (*AVR1–AVR7*; Keinanen *et al.*, 1994; Laitinen *et al.*, 2002). Two of the genes, *AVR4* and *AVR5*, are identical in their coding sequences, exhibiting only a single nucleotide difference in their 5′-flanking region, whereas the others are 94–99% identical to each other (Keinanen *et al.*, 1994). It has not yet been fully established whether or not the *AVR* genes are expressed as viable proteins in the chicken. The AVR proteins have previously been expressed artificially in various host-cell systems and their properties have been examined (Laitinen *et al.*, 2002; Hytönen *et al.*, 2004). Only the AVR4 and AVR5 (previously denoted as AVR4/5 and henceforth as AVR4) gene products have been shown to exhibit binding affinities towards biotin and 2-iminobiotin that are comparable to those of streptavidin yet somewhat weaker than those observed for avidin (Hytönen *et al.*, 2004). The amino-acid sequence of AVR4 shows 79 and 43% similarity (77 and 35% identity) to avidin and streptavidin, respectively (Fig. 1). In addition, AVR4 has shown increased thermal stability compared with avidin and streptavidin in both the apo and biotin-complexed forms (Hytönen *et al.*, 2004).

In the present study, we have determined the three-dimensional structures of AVR4 in the apo and the biotin-complexed forms and have compared them with the homologous structures in avidin and streptavidin. Based on detailed comparative analyses of the hydrogen-bonding interactions and the alterations in size and conformation of the critical L3,4 loop, we have interpreted the differences in the biotin-binding affinities between AVR4, avidin and streptavidin. In addition, we provide insight into the hyperthermostable properties of the three proteins regarding the exceptionally high stability of AVR4 with respect to avidin and streptavidin. In this context, differences in the structural determinants were identified that stabilize the tetrameric assembly of the protein and have a causative impact on thermostability. The results suggest that the phenomenon of thermostability may bear relevance not only to proteins derived from thermophilic microorganisms but can also be extended to higher order eukaryotic systems (*i.e.* vertebrates).

2. Materials and methods

2.1. Expression and purification of AVR4

Unlike the other *AVR* genes, the product of the *AVR4* gene contains a cysteine residue at position 122, which was converted to a serine in this work in order to avoid formation of undesired intermonomeric disulfide bridges. The resultant

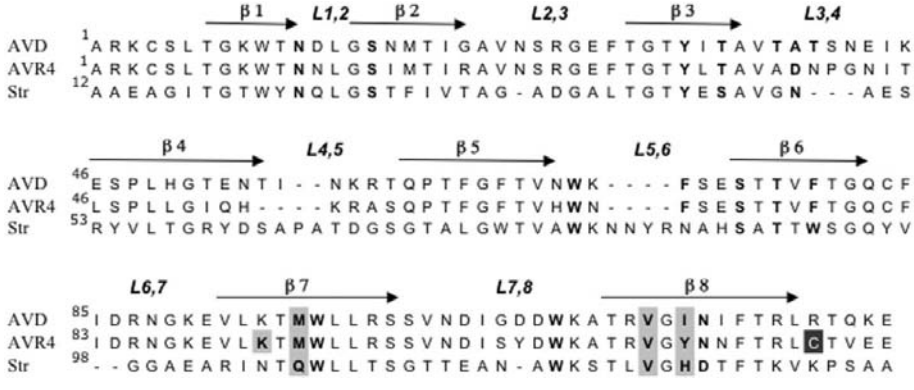

Figure 1
Structure-based sequence alignment of avidin, AVR4 and streptavidin. The position of the C122S mutation is highlighted in black. The secondary-structure β-strand elements are indicated by arrows and labelled and positions of the interconnecting loops are designated. Amino-acid residues that participate in biotin binding are shown in bold and residues that participate in the 1–3 monomer–monomer interaction are displayed in bold and highlighted in light grey.

C122S mutant displays near-identical biotin-binding and high thermal stability properties compared with those of the wild-type protein (Hytönen *et al.*, 2004). Thus, the C122S mutant protein served as the experimental model in this work and, unless otherwise stated, reference to AVR4 henceforth in the article represents this mutant. AVR4 was expressed in two different host-cell systems. In one, the AVR4 protein was produced using the Bac-To-Bac baculovirus expression system (Invitrogen) in Sf9 insect cells using biotin-free medium as described previously (Laitinen *et al.*, 2002). The expressed protein was purified by affinity chromatography using a 2-iminobiotin column as reported previously (Laitinen *et al.*, 2001). For the purposes of the present communication, this form of the protein is termed baculovirus-expressed AVR4. In another approach, AVR4 was expressed in an *Escherichia coli* host-cell system and purified by 2-iminobiotin affinity chromatography as previously reported (Hytönen *et al.*, 2004). The latter form is here termed bacteria-expressed AVR4.

2.2. Crystallization and data collection of baculovirus-expressed AVR4–biotin complex

Crystals of baculovirus-expressed AVR4–biotin complex were obtained by the hanging-drop vapour-diffusion method at 293 K. D-Biotin (Sigma B4501) was complexed with AVR4 prior to crystallization assays. A 4 µl drop containing equal volumes of protein solution (7.5 mg ml^{-1}) and reservoir solution (2 *M* ammonium sulfate, 0.1 *M* sodium acetate pH 4.6 with or without 10% glycerol) was used. The crystals were initially soaked in a cryoprotectant solution containing 2.0 *M* ammonium sulfate, 0.1 *M* sodium acetate pH 4.6 and 25% glycerol. Crystallographic data were collected at 100 K using an Oxford Cryosystems Cryostream cooling device from a single crystal on an ADSC Quantum 4R CCD detector with an oscillation range of 0.5° at beamline ID14-2 (λ = 0.933 Å) at the European Synchrotron Radiation Facility (ESRF), Grenoble, France. The crystal belonged to the tetragonal space group $P4_12_12$, with unit-cell parameters a = 80.96, c = 140.70 Å. Data were integrated, reduced and scaled using the *HKL* suite (Otwinowski & Minor, 1997).

2.3. Crystallization and data collection of bacteria-expressed AVR4

The bacteria-expressed AVR4 was crystallized in the native and biotin-complexed forms *via* the hanging-drop vapour-diffusion method with the reservoir solution containing 25–30% PEG 400, 0.1 *M* Tris buffer pH 8.5 and 0.2 *M* sodium citrate. The diamond-shaped crystals reached a size of 0.5 mm in the long dimension within 2 d but exhibited poor diffraction (8–10 Å maximal resolution). Better diffracting crystals with similar morphology were obtained using different crystallization conditions in which the reservoir solution contained 1.7–2.3 *M* sodium formate, 0.1 *M* sodium acetate pH 4.2. Biotin was complexed to AVR4 prior to crystallization by adding a saturated solution of the vitamin to the protein solution. Crystals of the native and biotin-complexed AVR4s were obtained within 2 d and reached final dimensions of 0.4–0.6 mm within 4 d. Diffraction data of both the native and biotin-complexed crystals were collected from a single crystal at 100 K on an ADSC Quantum 4R CCD detector with an oscillation range of 0.5° at beamline ID14-4 at the ESRF (λ = 0.9393 Å) using an Oxford Cryosystems Cryostream cooling device. The cryoprotectant solution contained 2.2 *M* sodium formate, 0.1 *M* sodium acetate buffer pH 4.6 and 25–30% glycerol. Data were integrated and scaled

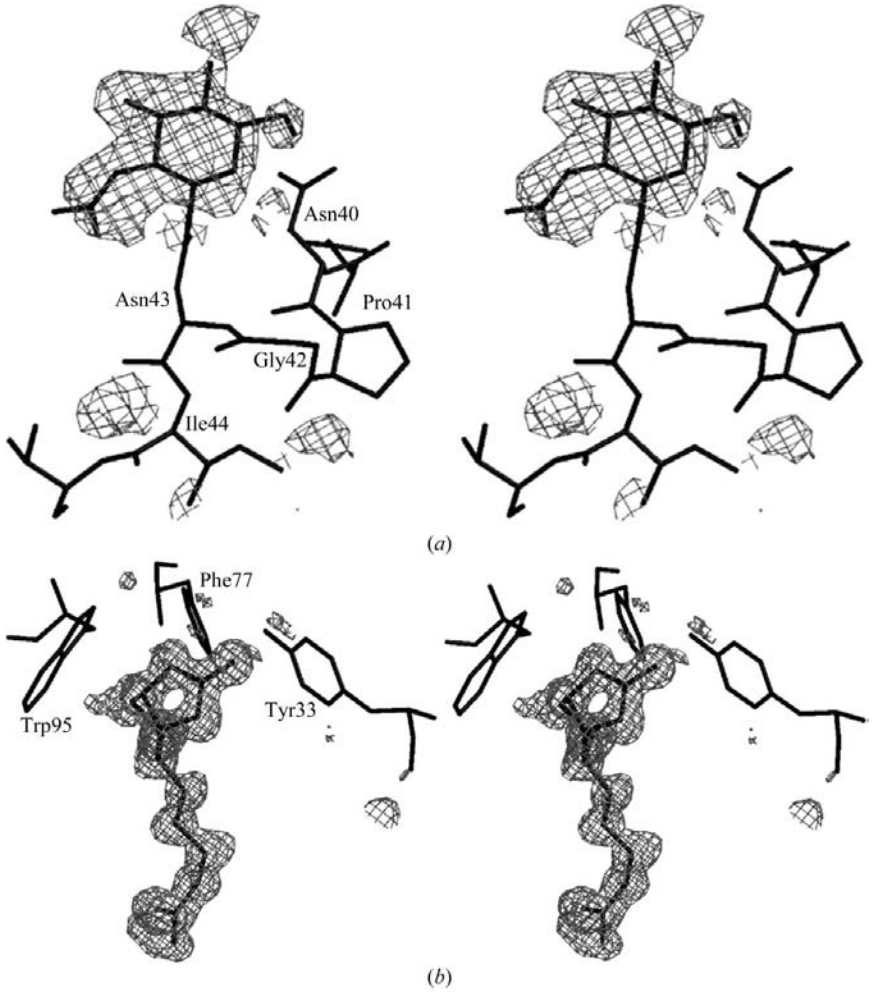

Figure 2
Electron-density maps of the baculovirus-expressed (*a*) and bacteria-expressed (*b*) AVR4–biotin complexes. (*a*) Stereoview of the $F_o - F_c$ electron-density map calculated at a resolution of 40.0–1.7 Å after the initial stage of refinement, displaying a segment of the L3,4 loop centred on the glycosylation site Asn43. All maps were constructed at 2.0σ with superimposed coordinates from the final models. (*b*) Difference map of the AVR4 biotin-binding site calculated in the resolution range 40–1.0 Å after the initial stage of refinement with no ligand in the model.

Table 1
Data-collection and refinement statistics.

Values in parentheses are for the outer shell.

	Baculovirus-expressed AVR4–biotin complex	Bacteria-expressed AVR4–biotin complex	Bacteria-expressed AVR4
Space group	$P4_12_12$	$P4_12_12$	$P4_12_12$
Unit-cell parameters (Å)	a = 80.96, c = 140.70	a = 78.04, c = 110.80	a = 78.04, c = 110.03
Resolution range (Å)	40–1.7 (1.73–1.7)	40–1.0 (1.02–1.0)	40–1.2 (1.22–1.2)
Unique reflections	51814	183076	107239
Redundancy	5.5	8.4	6.6
$R_{sym}(I)$†	4.6 (43.1)	5.4 (43.6)	6.5 (48.1)
Completeness	99.5 (99.9)	98.5 (88.1)	99.8 (99.6)
$I/\sigma(I)$	22.6 (1.8)	32.5 (1.3)	25.53 (3.66)
No. of protein atoms	1895	1976	1897
No. of ligand atoms	32	32	0
No. of carbohydrate atoms	56	0	0
No. of solvent atoms	121	240 water + 12 formate	171 water + 18 formate
R factor (%)	19.2	16.6	17.7
R_{free}‡	20.0	17.7	18.5
Average B factor (Å^2)			
Protein	32.5	11.9	14.3
Ligand	25.1	8.7	0
Carbohydrate	55.8	—	—
Solvent	39.2	23.1 (water)/ 15.9 (formate)	22.1 (water)/ 20.5 (formate)
R.m.s.d. from ideality			
Bond length (Å)	0.014	0.014	0.011
Bond angle (°)	1.65	1.72	1.4
Ramachandran plot (*PROCHECK*)			
Favoured (%)	93.3	94.3	93.8
Allowed (%)	6.7	5.7	6.2
Generously allowed (%)	0.0	0.0	0.0
Disallowed (%)	0.0	0.0	0.0

† $R_{sym}(I) = \sum |I - \langle I \rangle| / \sum I$. ‡ Test set is 5% for all data.

using the *HKL* suite (Otwinowski & Minor, 1997). The crystals belonged to space group $P4_12_12$, with unit-cell parameters a = 78.04, c = 110.8 Å, and a = 78.04, c = 110.03 Å for the native and the biotin complex, respectively, with two monomers in the asymmetric unit. The values for the c axis were substantially shorter than that of the baculovirus-expressed glycosylated AVR4 (see §3.2).

3. Results

3.1. Structure determination of baculovirus-expressed AVR4

The structure of AVR4 was solved *via* the molecular-replacement method using *AMoRe* (Navaza, 1994) as implemented in the *CCP*4 suite (Dodson *et al.*, 1997) using avidin (PDB code 2avi) as the search model. The solution in *AMoRe* resulted in an R value of 40.0% and a correlation coefficient of 58.2% at a resolution range of 15.0–4.0 Å. There are 26 differences in the sequence between avidin and AVR4 (Fig. 1). These mutations were inserted into the model using the graphics program *O* (Jones & Kjeldgaard, 1997). The structure was further refined using *REFMAC*5 (Murshudov *et al.*, 1997) as implemented in *CCP*4*i* (Potterton *et al.*, 2003) using the rigid-body protocol followed by restrained refinement with the maximum-likelihood option in the resolution range 40.0–1.7 Å. The initial electron-density maps calculated after the first five cycles of restrained refinement indicated the presence of biotin molecules in the binding sites. There are three possible glycosylation sites on AVR4 (Laitinen *et al.*, 2002), two of which, Asn43 and Asn117, could be assigned based on the electron-density map (Fig. 2*a*). In addition, there was a clear indication that the L3,4 loop has a different conformation compared with that observed in the avidin–biotin complex; the loop residues were thus removed prior to the next cycle of refinement. The resultant electron-density maps ($F_o - F_c$ and $2F_o - F_c$) were extremely clear and all of the L3,4 residues were traced successfully. The carbohydrate moieties of the baculovirus-expressed AVR4 were not analyzed and the asparagine-linked residue was assigned as *N*-acetyl glucosamine (GlcNAc). The structure was further refined in the resolution range 40–1.7 Å using *REFMAC*5 and solvent molecules were added utilizing *ARP*/*wARP* (Lamzin & Wilson, 1993) (Table 1). The structure was fitted into electron-density maps using the graphics program *O* (Jones & Kjeldgaard, 1997). The model of the baculovirus-expressed biotin–AVR4 complex consists of residues 3–122 for monomers 1 and 2, with two biotin molecules, four GlcNAc molecules and 121 solvent molecules. The coordinates and structure factors (PDB code 1y52) have been deposited in the PDB (Berman *et al.*, 2002).

3.2. Structure determination of bacteria-expressed AVR4

The structure of the AVR4–biotin complex was solved *via* molecular-replacement methods using *AMoRe* (Navaza, 1994) as implemented in the *CCP*4 suite (Dodson *et al.*, 1997), with the refined baculovirus-expressed AVR4 as the search model after removing solvent, ligand and carbohydrate molecules. The solution in *AMoRe* resulted in an R value of 40.8% and a correlation coefficient of 52.8% in the resolution range 15.0–4.0 Å. The initial ($F_o - F_c$) and ($2F_o - F_c$) electron-density maps calculated after the first five cycles of restrained refinement indicated the presence of biotin molecules in the binding sites (Fig. 2*b*). The structure was further refined in the resolution range 50–1.0 Å using *REFMAC*5 and solvent molecules were added utilizing *ARP*/*wARP* (Lamzin & Wilson, 1993). The structure was built into electron-density maps using the graphics program *O* (Jones & Kjeldgaard, 1997). The AVR4–biotin complex consists of residues 3–122 for both monomers, two biotin molecules, 240 solvent and four formate molecules (Table 1).

The space group and unit-cell parameters of the apo-AVR4 were virtually identical to those of the biotin complex and the structure was refined using the rigid-body protocol in *REFMAC*5 (Murshudov *et al.*, 1997). The initial difference electron-density maps indicated that the binding site contains two formate anions and two solvent molecules in the respective asymmetric unit monomers. The structure was further refined using *REFMAC*5 restrained refinement with the maximum-likelihood option and solvent molecules were added utilizing *ARP*/*wARP* (Lamzin & Wilson, 1993). The model of apo-AVR4 consists of residues 3–122 for monomers 1 and 2, with four formate molecules and 171 solvent molecules (Table 1). The models of the apo and biotin-complexed AVR4 (PDB codes 1y53 and 1y55, respectively) are available from the PDB (Berman *et al.*, 2002).

3.3. Structure of AVR4

The overall tertiary and quaternary structures of AVR4 show high similarity to those of avidin and streptavidin (Hendrickson *et al.*, 1989; Weber *et al.*, 1989; Livnah *et al.*, 1993). The tertiary structure consists of eight antiparallel β-strands that form a β-barrel. The quaternary structure comprises a dimer of dimers as previously proposed for avidin and streptavidin (Kurzban *et al.*, 1991). The tertiary structures of both the baculovirus-expressed and bacteria-expressed

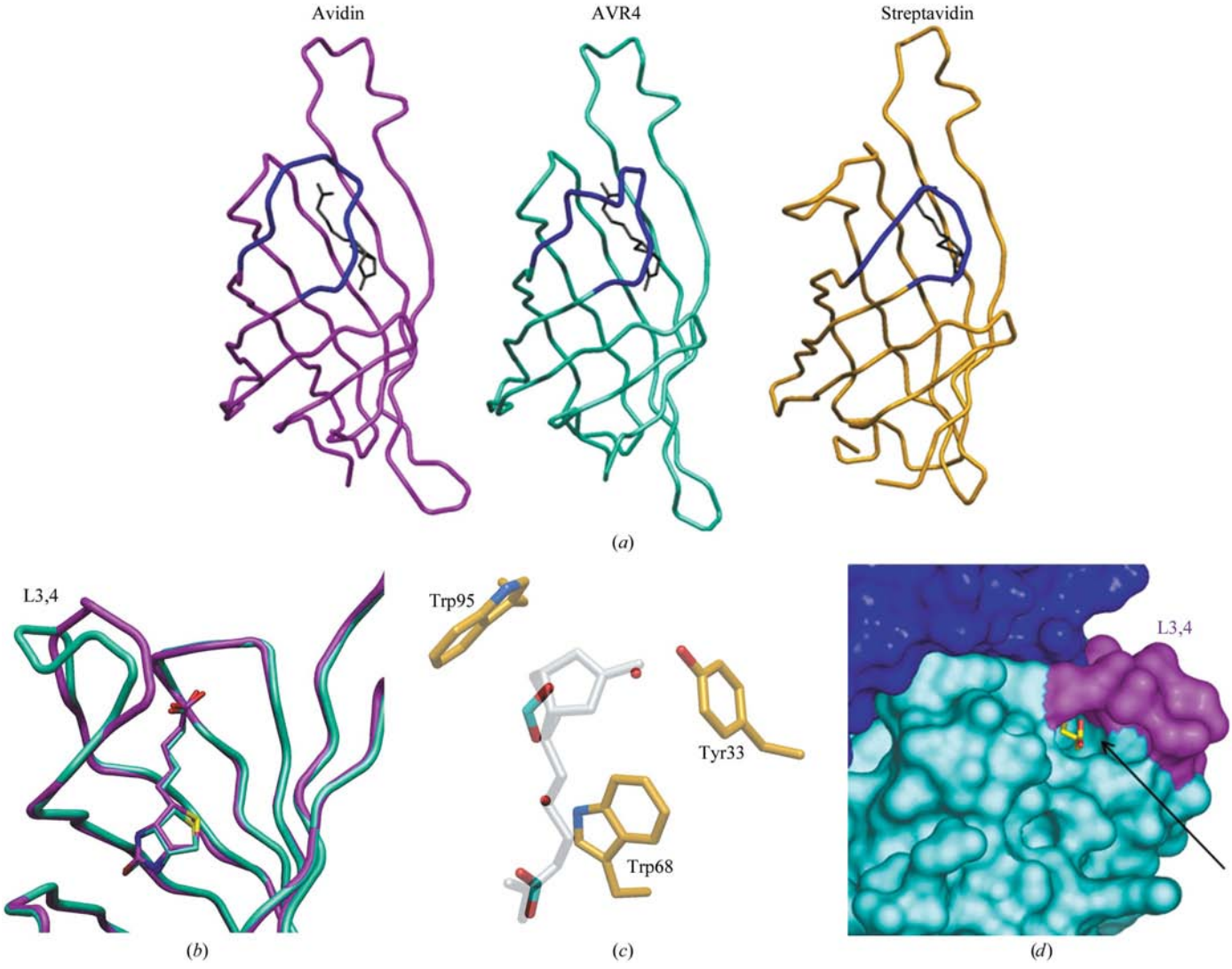

Figure 3
(*a*) Tube representation of the monomeric structure of avidin (magenta), AVR4 (cyan) and streptavidin (gold). The L3,4 loop is coloured blue, indicating its different size and conformation in the three proteins. Biotin is shown in black in the respective binding site. (*b*) Superposition of avidin and AVR4 in the L3,4 loop region. One can clearly observe the entirely different conformation of the respective loop (labelled) despite the identical length. (*c*) Biotin-binding site of apo-AVR4. The two water and two formate molecules in the site emulate the structure of biotin (superimposed in semi-transparent light grey). Selected aromatic residues are shown in gold and labelled. (*d*) Surface presentation of the biotin-binding region of AVR4. The adjacent monomer forming the 1–2 interaction is shown in dark blue and the surface formed by the amino-acid residues of the L3,4 loop is rendered in magenta. The carboxylate moiety of biotin (shown in yellow) is completely exposed to solvent and the portal cavity formed by the conformation of the L3,4 loop is indicated by an arrow.

AVR4–biotin complexes are highly similar, with no significant differences in the conformations of the hairpin-loop regions and the biotin-binding site. Superposition of monomers 1 and 2 of the baculovirus-expressed and bacteria-expressed AVR4–biotin complexes resulted in low r.m.s.d.s of 0.14 and 0.18 Å, respectively (for 114 C^{α} pairs). The N-linked carbohydrate moieties in the baculovirus-expressed AVR4 at positions Asn43 (L3,4 loop) and Asn117 (β8 strand) have no apparent effect on the protein structure. Thus, owing to the high resolution of the bacteria-derived crystals, the subsequent structural analysis and comparison of the AVR4 model are based on the bacteria-expressed protein.

Superposition of the tertiary structures of AVR4 and avidin results in a relatively low r.m.s.d. of 0.36 Å (for 103 C^{α} pairs). The entire β-barrel scaffold is highly similar in both proteins and the largest differences between the structures occur in several of the loop regions. The loop connecting β4 and β5 (L4,5) is two residues shorter in AVR4 with a different amino-acid composition (Fig. 1) and the loop assumes an entirely different conformation. The respective L6,7 loops of avidin and AVR4 also exhibit different conformations, although the sequences of both proteins are identical in this vicinity. In this context, L6,7 has been shown to be of high flexibility in many avidin structures and in some cases is partially disordered (Pazy *et al.*, 2002).

In both the avidin–biotin and AVR4–biotin complexes, the crucial lid-like L3,4 loops (residues 35–46) are in a closed and ordered conformation but adopt an entirely different structure (Fig. 3*a*). Although the respective L3,4 loops are of the same length in both proteins, differences in amino-acid composition dictate the variation in the corresponding loop conformation (Figs. 1 and 3*a*). In AVR4, the presence of a distinctive proline-glycine tandem pair at positions 41 and 42 (respective φ, ψ values of -64, -21° and -64, -16°) induces rigidity in the loop and forms a 'kink' resembling a short helical segment (Fig. 3*b*). In addition, Asp39 forms an intramonomeric salt-bridge interaction with Arg112 from β8 (not shown), thereby enhancing the conformational stability of L3,4. In the apo-AVR4 structure, two solvent and two formate molecules (originating from the crystallization solution) occupy the biotin-binding pocket. These molecules emulate the biotin contour and also form similar interactions with the protein (Fig. 3*c*). Interestingly, one of the formate molecules assumes a position almost identical to that of the biotin carboxylate group and forms similar hydrogen-bonding interactions. Notably, unlike the disordered conformation of the L3,4 loop in both apo-streptavidin and apo-avidin, the corresponding loop in the apo-AVR4 form is in the closed and ordered conformation, similar to that observed in the AVR4–biotin complex. In both the apo and biotin-complexed AVR4 structures the L3,4 loop forms a 'portal' cavity at the entrance of

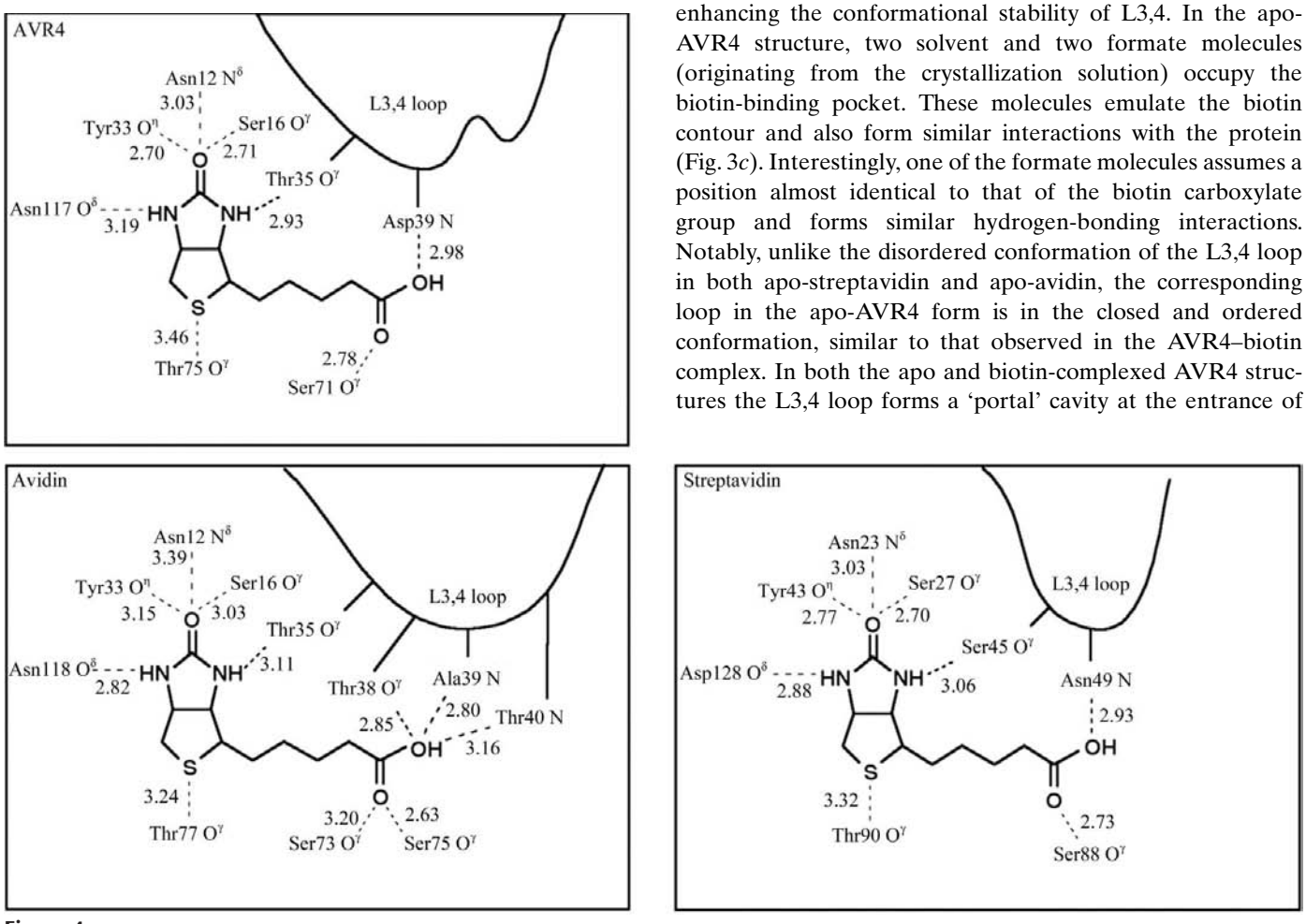

Figure 4
Schematic representation of the hydrogen-bonding network in the avidin, AVR4 and streptavidin complexes with biotin. In all three proteins, the fused biotin-ring system forms an identical network of hydrogen-bonding interactions. In addition, the L3,4 loop forms a single hydrogen-bonding interaction with one of the biotin ureido N atoms. In contrast, there are differences in the interactions of the biotin carboxylate with the respective proteins. In the avidin–biotin complex, one of the carboxylate O atoms forms three hydrogen bonds with Thr38 O^{γ}, Ala39 N and Thr40 N and the other forms two hydrogen bonds with Ser73 O^{γ} and Ser75 O^{γ}. In AVR4, the L3,4 loop is the same length as in avidin, yet a different conformation is displayed owing to its altered amino-acid composition. Consequently, one of the biotin carboxylate O atoms interacts with one hydrogen bond and the other forms a hydrogen bond with Ser71 O^{γ} (analogous to Ser73 of avidin). In streptavidin, there are also two hydrogen-bonding interactions between the biotin carboxylate O atoms and the protein, such that one forms a hydrogen bond with Asp49 N and the other with Ser88 O^{γ} (analogous to Ser75 of avidin).

the biotin-binding site. This cavity is sufficiently spacious to permit biotin binding without any alterations in the loop conformation. In the AVR4–biotin complex, the carboxylate moiety of biotin is thus completely exposed to solvent, as shown in Fig. 3(*d*).

The overall polar and hydrophobic interactions of biotin with avidin, streptavidin and AVR4 are quite similar. In AVR4, the five hydrophobic core residues (two Phe and three Trp residues) which accommodate biotin are identical to those in avidin (Livnah *et al.*, 1993). In streptavidin, the composition of the hydrophobic core residues is somewhat different, comprising four Trp residues (Hendrickson *et al.*, 1989; Weber *et al.*, 1989). The biotin bicyclic ring system forms an identical hydrogen-bonding network with all three proteins (Fig. 4). In contrast to these similarities, the hydrogen-bonding interactions of the biotin carboxylate are different for the three proteins. As reported earlier (Livnah *et al.*, 1993), a total of five hydrogen bonds are formed between the biotin carboxylate and avidin, compared with only two in the complex with streptavidin. Subtler differences are observed for the interaction of the biotin carboxylate O atoms with AVR4. Two hydrogen bonds are formed, similar to the interaction with streptavidin, but the hydrogen bond with Ser71 O^{γ} is equivalent to that of Ser73 of avidin instead of Ser88 of streptavidin (Fig. 4).

3.4. Comparative quaternary structure of AVR4

The quaternary assembly of AVR4 essentially reflects the previously suggested dimer-of-dimers arrangement (Kurzban *et al.*, 1991) of avidin and streptavidin (Fig. 5*a*). Each dimer is composed of the tight 1–4 monomer–monomer interaction (Livnah *et al.*, 1993), wherein the two AVR4 monomers form a sandwich-like structural dimer with a substantial contact surface (Table 2). The contrasting dimer–dimer interface comprises the combined contribution of the 1–2 and 1–3 monomer–monomer interactions. The functional 1–2 interaction in AVR4 is similar to that of avidin and streptavidin, consisting mainly of the contribution of Trp108 (equivalent to Trp110 and Trp120 in avidin and streptavidin, respectively; Fig. 1). As in avidin and streptavidin, Trp108 is donated from an adjacent subunit to the biotin-binding pocket, which explains why the tetrameric assembly of AVR4 is further stabilized upon biotin binding (Table 2).

The 1–3 monomer–monomer interface appears to be part of a 'weak link' in the quaternary structures of both avidin and streptavidin, since only three residues of each subunit participate in this intermonomer interaction. In contrast, the equivalent interface of AVR4 reflects the contribution of four residues, three of which occur in equivalent positions to those of avidin and streptavidin, *i.e.* Met94 from strand β7 of AVR4 and Val113 and Tyr115 from strand β8 (Fig. 5). In AVR4, the two Tyr115 side chains stack together (3.85 Å) to form a $\pi-\pi$ (charge-transfer) interaction. In addition, Lys92 N^{ζ} (the fourth residue) from strand β7 crosses over from one monomer and forms a hydrogen-bonding interaction with the adjacent Tyr115 O^{η} (3.09 and 3.34 Å for the biotin complex and apo structures, respectively). Lysine is known to serve as a donor of three potential hydrogen-bonding interactions, while the tyrosine hydroxyl group can exhibit both donor and/or acceptor potential (Ippolito *et al.*, 1990). The 1–3 interface is further stabilized by an intricate network of interactions involving water molecules, which collectively appear to mitigate the interaction between two potential electron donors (Fig. 5). In this context, Lys92 also forms an intramonomeric hydrogen-bonding interaction with Asn117 O^{δ}, thus stabilizing the conformation of its side chain, and with a water molecule, forming a total of three hydrogen-bonding interactions. In addition, Tyr115 contains an additional hydrogen-bonding interaction with a water molecule (Fig. 5). Although in avidin the corresponding lysine residue (Lys94) is conserved, such an intricate network of interactions is absent, since a hydrogen-bonding counterpart (*i.e.* a Tyr115 equivalent) is lacking. As a consequence of Tyr115 and Lys92, the dimer–dimer interface in AVR4 is significantly larger than those calculated for avidin and streptavidin (Table 2).

4. Discussion

The avidin gene represents one of a family of avidin-related genes in the chicken genome. Interestingly, only the protein derived from the avidin gene is so far known to be expressed under normal conditions. The function of the other avidin-related genes remains an enigma and it is interesting to speculate whether they may carry an innate disadvantage that prevents their expression. In this work, we describe the high-resolution structures of the avidin-related protein AVR4 in the apo and biotin-complexed forms. Comparison of the latter AVR4 structures with those of streptavidin and avidin reveals the basis for the observed differences in both their binding affinities towards biotin and their thermostability properties.

The primary structure of AVR4 is highly homologous to those of streptavidin and particularly avidin (Fig. 1) and most of the biotin-binding residues are conserved in the three proteins. The binding affinities of AVR4 for biotin and 2-iminobiotin are somewhat lower than avidin but similar to those of streptavidin (Table 2; Hytönen *et al.*, 2004). The relatively lower affinity of AVR4 towards biotin compared with avidin can be attributed both to the number of interacting residues and to the conformation of the L3,4 loop. For avidin and AVR4, the hydrophobic 'cage' comprising five aromatic residues is identical; the major difference in the biotin-binding pocket reflects the number of hydrogen-bonding interactions between the biotin carboxylate (Fig. 4). In AVR4 and streptavidin, there are only two hydrogen-bonding interactions with the biotin carboxylate as opposed to five in avidin. The number of the respective hydrogen-bonding interactions is a function of both the length and the conformation of the L3,4 loop. In streptavidin, for example, the shorter L3,4 loop contributes only a single hydrogen-bonding interaction with the biotin carboxylate (Fig. 4). This lid-like L3,4 loop has been shown to play a crucial role in the high binding affinity towards biotin; removal of the loop in streptavidin by circular permutation resulted in a substantial decrease in K_a to a value

Table 2
Comparative binding, thermal stability and contact-surface data of AVR4, avidin and streptavidin.

	Ligand binding (M)		Stability		Contact surface area† (Å^2)			
	K_d, biotin	K_d, 2-iminobiotin‡	T_m without biotin§ (K)	T_m with biotin§ (K)	Dimer–dimer	1–3 monomer–monomer	1–4 monomer–monomer	1–2/3/4 monomer–trimer
AVR4(C122S)	3.6×10^{-14}	1.1×10^{-7}	379.5	398.5	1531	235	1620	2400
Avidin	1.1×10^{-16}	2.2×10^{-8}	356.6	390.1	1414	158	1850	2561
Streptavidin	4.0×10^{-14}	1.7×10^{-7}§	348.6/355.4¶	385.8	1344	186	1536	2222

† All contact surfaces were calculated for the corresponding biotin complexes using the protein–protein interaction server (Jones & Thornton, 1996). The values indicate the contact surface of a single partner. The values in parentheses represent the polar to hydrophobic ratio of the contact surfaces. ‡ Affinity to 2-iminobiotin surface calculated from equilibrium response data (Hytönen *et al.*, 2004). § Laitinen (personal communication). ¶ The differences in these results are suggested to be related to the differences in the quality of commercial streptavidin according to Waner *et al.* (2004). However, the conditions used in the experiments are not fully identical.

of $10^7\ M^{-1}$ (Chu *et al.*, 1998), indicating that in the native biotin-complexed structure the closed conformation of the loop also shields much of the ligand in the binding site from solvent. However, owing to the relatively small size of the L3,4 loop in streptavidin, the closed conformation leaves the carboxylate portion of biotin completely exposed to solvent. Although the L3,4 loop of the avidin–biotin complex also assumes a closed conformation, the ligand is almost completely buried in the binding pocket, in which three hydrogen-bonding interactions are formed with one of the biotin carboxylate O atoms (Fig. 4). In contrast to both avidin and streptavidin, the L3,4 loop of AVR4 exhibits an alternative conformation. The loop is the same length as in avidin and three residues longer than streptavidin. Nevertheless, owing to its divergent conformation the ligand is exposed to solvent and only a single hydrogen bond is formed with the biotin carboxylate moiety (Figs. 3*d* and 4).

The rate of association in the avidin–biotin complex is similar to that of many other protein–ligand interactions and the crucial factor for the high affinity constant appears to mainly reflect the extremely slow rate of dissociation (Green, 1990). Taken together, the number of hydrogen-bonding interactions and the availability of the ligand to solvent can account for the observed differences in binding affinities. Examination of the amino-acid sequences of other members of the AVR family reveals that the L3,4 is highly conserved as is the presence of the Pro-Gly pair (Laitinen *et al.*, 2002). In this context, it may be concluded that the unique structural features of the L3,4 loop in all AVR family members are highly similar and, consequently, the interactions of the L3,4 loop with the biotin carboxylate and its availability to solvent would be identical to those observed in the model for AVR4.

Avidin and streptavidin are regarded as hyperthermostable in their apo forms and the proteins display an increase in their T_m when bound to biotin (Table 2; Gonzalez *et al.*, 1999; Waner *et al.*, 2004). Unlike avidin and streptavidin, however, AVR4 displays hyperthermostable properties even in its apo form and exhibits exceptional stability upon biotin binding (Table 2; Hytönen *et al.*, 2004, 2005). The factors and structural determinants that induce thermostability in proteins have been subjected to extensive investigation and it is achieved by subtle differences residing over the entire molecule without substantial alterations in the protein fold (Matthews *et al.*, 1974; Perutz & Raidt, 1975; Zuber, 1988; Scandurra *et al.*, 1998; Criswell *et al.*, 2003). The latter studies have indicated that features such as better or tighter atom packing, the ratio between the polar surface and buried hydrophobic surface areas, salt-bridge formation and higher content of proline residues are all considered to influence the thermostability of a protein (Scandurra *et al.*, 1998; Kumar & Nussinov, 1999, 2001; Vieille & Zeikus, 2001). Despite these general observations, each case of a thermostable protein must be evaluated individually in reference to biochemical and structural data.

Salt-bridge interactions are considered to be a prominent factor that can enhance thermostability in proteins (Vetriani *et al.*, 1998; Yip *et al.*, 1998; Bogin *et al.*, 2002). In the case of AVR4, avidin and streptavidin, it is quite evident that the number of salt-bridge interactions does not play a significant role in heightened thermostability, since AVR4, the most thermostable protein of the three (Table 2), has the lowest number of salt-bridge interactions (three) per subunit compared with avidin (seven) and streptavidin (four).

Proline, which can adopt only a limited number of conformations in a polypeptide chain, has the lowest conformational entropy. The presence of proline residues in loop regions of a protein is considered to induce rigidity and to thus contribute to protein thermostability (Delboni *et al.*, 1995; Bogin *et al.*, 1998; Vieille & Zeikus, 2001). In avidin and streptavidin there are two proline residues, one of which is in the loop region of L4,5 (Fig. 1). In AVR4, however, there is an additional exposed proline residue in the L3,4 loop which contributes to its stable conformation. In addition, as described in §3, the L3,4 loop is further stabilized by a salt bridge (between Asp39 and Arg112). In this context, loop rigidity has also been shown to contribute to the thermal properties of proteins (Russell *et al.*, 1997; Vieille & Zeikus, 2001). Unlike avidin and streptavidin, the L3,4 loop of AVR4 maintains its conformation in both the apo and biotin-complexed forms and L3,4 stability may partially account for the differences in the respective T_m values of the three proteins (Table 2). Thus, the L3,4 loops of avidin and streptavidin are highly flexible in their apo forms and the differences in T_m are 30 K higher in the biotin-complexed forms in which the loops are closed. In contrast, the L3,4 loop of apo-AVR4 is already in the closed conformation; the T_m is already very high and the difference between the apo and biotin-complexed forms is only 292 K (Table 2).

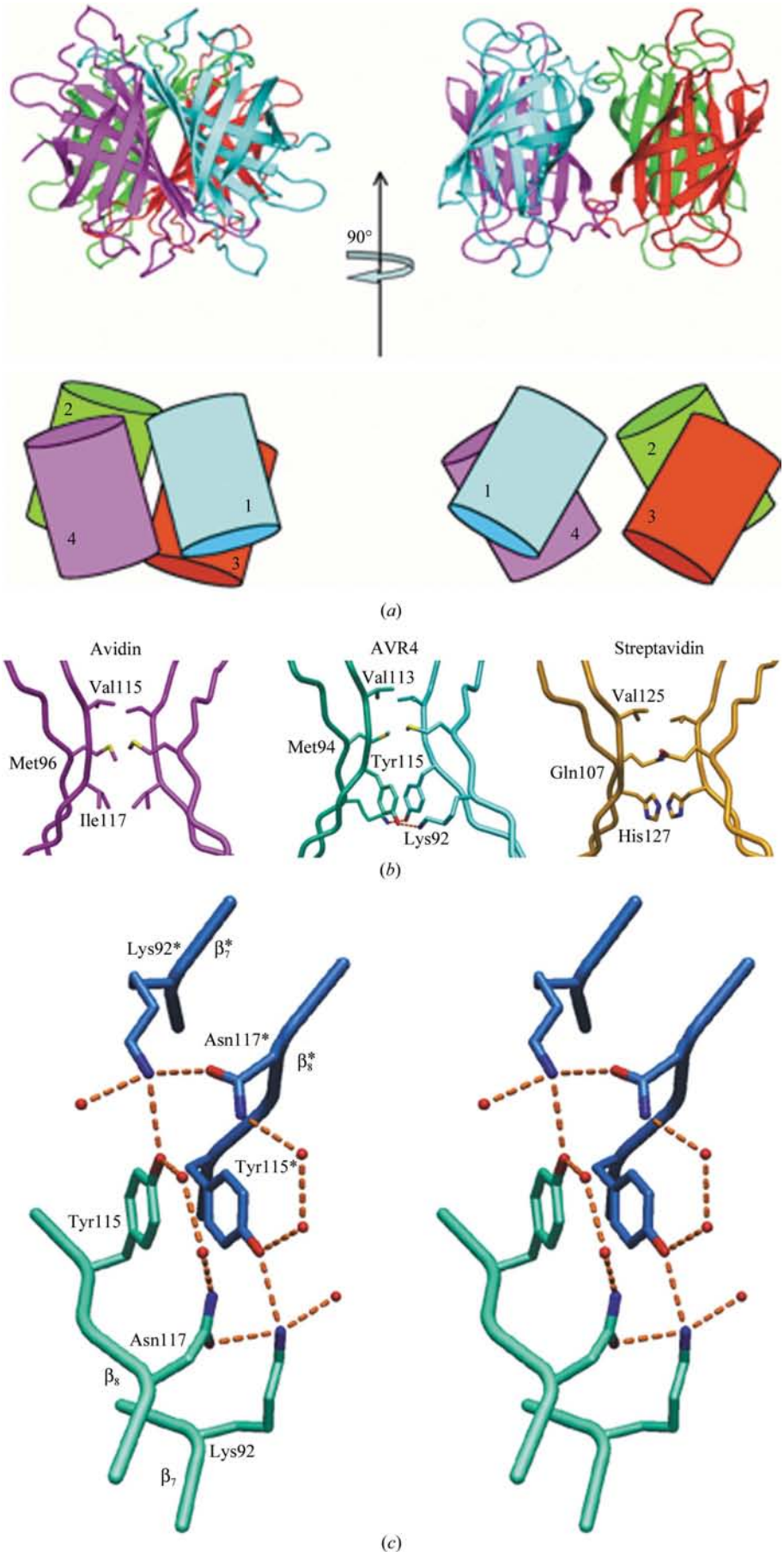

Recent studies have shown that transferring the L3,4 loop from AVR4 into avidin resulted in a substantial increase in T_m values of the mutants (Hytönen *et al.*, 2005).

Finally, in oligomeric proteins the chemical nature and the extent of the subunit–subunit interfaces may have a pronounced effect on thermostability (Korkhin *et al.*, 1999; Gerk *et al.*, 2000). Analysis of the contact-surface interaction shows that the monomers of each of the three proteins exhibit a substantial contact surface with the other three subunits (Table 2). In addition, the contact surface of each subunit of the 1–4 structural dimer is larger than the complementary dimer–dimer interface contributed by the combined 1–2 and 1–3 interactions. Based on these data, it appears unlikely that a single monomer will dissociate directly from the tetrameric

Figure 5
Intersubunit interactions of AVR4. (*a*) Schematic presentation of the quaternary structure of avidin, AVR4 and streptavidin. The ribbon diagram (top) is depicted from the avidin coordinates and the cartoon (bottom) represents the relative arrangement of the monomers (numbered) in all three proteins. The tetramer on the right is rotated clockwise by 90° along the vertical axis. The intimate interaction of the 1–4 (and 2–3) monomer–monomer interface is clearly visible in the figure on the left. The contact surface of the alternative interface, comprising the dimer–dimer interaction (right), is much less extensive. (*b*) The 1–3 interface of avidin (magenta), AVR4 (cyan) and streptavidin (gold). The intersubunit interactions involve only three residues in avidin and streptavidin, although their character is somewhat different (*e.g.* the interaction in avidin is more hydrophobic than that of streptavidin). In contrast, the 1–3 contact surface of AVR4 contains the additional contribution of a fourth amino-acid side chain (Lys92), which crosses over from one monomer and forms a hydrogen-bonding interaction with Tyr115 of the other. (*c*) Close-up stereoview of the intricate hydrogen-bonding network between Lys92 and Tyr115 in the 1–3 monomer–monomer interface. The different subunits are coloured cyan and blue, respectively. The two Tyr115 from the different monomers form a $\pi-\pi$ charge-transfer interaction with an angle of rotation of ~60° between the two rings. Lys92 of the neighbouring subunit forms a hydrogen-bonding interaction with Tyr115, which increases the 1–3 contact surface. In addition, Lys92 forms two additional hydrogen-bonding interactions with Asn117 and a solvent molecule.

assembly and the dissociation into subunits would presumably involve a discrete step in which the structure initially undergoes separation into the two 1–4 structural dimers. This phenomenon, combined with the relatively few residues that characterize the 1–3 interface in all three proteins, would presumably reflect a 'weak link' in the dimer–dimer arrangement (Table 2). Nonetheless, the 1–3 interface in AVR4 involves more extensive interactions compared with those of avidin and streptavidin and the correspondingly larger dimer–dimer contact surface correlates nicely with the respective T_m values (Table 2). The combined presence of the tyrosine–tyrosine charge-transfer and lysine–tyrosine hydrogen-bonding interactions largely accounts for this difference in the contact surfaces. It has been suggested that strategic placement of structural determinants at positions that enhance subunit interface is a significant promoter of enhanced thermostability (Korkhin *et al.*, 1999). In addition, aromatic stacking has been shown to play a significant role in enhancing the thermostability of proteins (Kannan & Vishveshwara, 2000; Park *et al.*, 2002). These data indicate that the increase and chemical nature of the dimer–dimer interactions are likely to make a substantial contribution to thermostability of AVR4. These findings have been recently substantiated experimentally by transferring Tyr115 from AVR4 into avidin, thus increasing the T_m (Hytönen *et al.*, 2005). Similarly, high thermostability properties would also be expected for other members of the AVR family (AVR3, AVR6 and AVR7), which also contain a tyrosine residue at position 115 (Laitinen *et al.*, 2002). Since all members of the AVR family contain a lysine residue at position 92, we would thus anticipate a similar network of 1–3 interactions in the latter AVRs as observed for AVR4 (Fig. 5*b*). Conversely, AVR1 and AVR2 both have an asparagine residue at position 115 which, based on preliminary modelling (not shown), would not be expected to contribute to the 1–3 contact surface as the tyrosine and these two members of the family would presumably exhibit reduced thermostability properties.

In conclusion, we have demonstrated that AVR4 is a hyperthermostable protein that indeed exhibits many of the features that characterize such proteins. The outstanding question is why would nature choose not to express the avidin-related proteins but instead chooses to express avidin, even though the *AVR* genes are present on the genome. Perhaps this phenomenon reflects an important role for the increased stability of a protein upon ligand binding (such as that observed for avidin upon binding biotin) and that expression of the AVRs may be induced under certain conditions (*e.g.* stress-related). In any case, our results provide new insight into the intramolecular forces that contribute to the thermostability of multimeric proteins. This information can extend the applications of the (strept)avidin–biotin system and can further contribute to the general design of hyperthermostable multimeric proteins.

The research was supported in part by the Israeli Science Foundation. We thank the staff of the ESRF, Grenoble, France for their assistance. We thank Irene Helkala, Eila Korhonen and Jarno Hörhä for their excellent technical assistance.

References

Bayer, E. A. & Wilchek, M. (1990). *J. Chromatogr.* **510**, 3–11.
Berman, H. M., Battistuz, T., Bhat, T. N., Bluhm, W. F., Bourne, P. E., Burkhardt, K., Feng, Z., Gilliland, G. L., Iype, L., Jain, S., Fagan, P., Marvin, J., Padilla, D., Ravichandran, V., Schneider, B., Thanki, N., Weissig, H., Westbrook, J. D. & Zardecki, C. (2002). *Acta Cryst.* D**58**, 899–907.
Bogin, O., Levin, I., Hacham, Y., Tel-Or, S., Peretz, M., Frolow, F., Burstein, Y., Korkhin, Y. & Kalb, A. J.. (2002). *Protein Sci.* **11**, 2561–2574.
Bogin, O., Peretz, M., Hacham, Y., Korkhin, Y., Frolow, F., Kalb, A. J. & Burstein, Y. (1998). *Protein Sci.* **7**, 1156–1163.
Chu, V., Freitag, S., Le Trong, I., Stenkamp, R. E. & Stayton, P. S. (1998). *Protein Sci.* **7**, 848–859.
Criswell, A. R., Bae, E., Stec, B., Konisky, J. & Phillips, G. N. Jr (2003). *J. Mol. Biol.* **330**, 1087–1099.
Delboni, L. F., Mande, S. C., Rentier-Delrue, F., Mainfroid, V., Turley, S., Vellieux, F. M., Martial, J. A. & Hol, W. G. (1995). *Protein Sci.* **4**, 2594–2604.
Dodson, E. J., Winn, M. & Ralph, A. (1997). *Methods Enzymol.* **277**, 620–633.
Freitag, S., Le Trong, I., Chilkoti, A., Klumb, L. A., Stayton, P. S. & Stenkamp, R. E. (1998). *J. Mol. Biol.* **279**, 211–221.
Freitag, S., Le Trong, I., Klumb, L., Stayton, P. S. & Stenkamp, R. E. (1997). *Protein Sci.* **6**, 1157–1166.
Gerk, L. P., Leven, O. & Muller-Hill, B. (2000). *J. Mol. Biol.* **299**, 805–812.
Gonzalez, M., Argaraña, C. E. & Fidelio, G. D. (1999). *Biomol. Eng.* **16**, 67–72.
Green, N. M. (1975). *Adv. Protein Chem.* **29**, 85–133.
Green, N. M. (1990). *Methods Enzymol.* **184**, 51–67.
Hendrickson, W. A., Pahler, A., Smith, J. L., Satow, Y., Merritt, E. A. & Phizackerley, R. P. (1989). *Proc. Natl Acad. Sci. USA*, **86**, 2190–2194.
Hytönen, V. P., Määtä, J. A., Nyholm, T. K., Livnah, O., Eisenberg-Domovich, Y., Hyre, D., Nordlund, H. R., Hörhä, J., Niskanen, E. A., Paldanius, T., Kulomaa, T., Porkka, E. J., Stayton, P. S., Laitinen, O. H. & Kulomaa, M. S. (2005). *J. Biol. Chem.* **280**, 10228–10233.
Hytönen, V. P., Nyholm, T. K., Pentikainen, O. T., Vaarno, J., Porkka, E. J., Nordlund, H. R., Johnson, M. S., Slotte, J. P., Laitinen, O. H. & Kulomaa, M. S. (2004). *J. Biol. Chem.* **279**, 9337–9343.
Ippolito, J. A., Alexander, R. S. & Christianson, D. W. (1990). *J. Mol. Biol.* **215**, 457–471.
Jones, S. & Thornton, J. M. (1996). *Proc. Natl Acad. Sci. USA*, **93**, 13–20.
Jones, T. A. & Kjeldgaard, M. (1997). *Methods Enzymol.* **277**, 173–208.
Kannan, N. & Vishveshwara, S. (2000). *Protein Eng.* **13**, 753–761.
Keinanen, R. A., Wallen, M. J., Kristo, P. A., Laukkanen, M. O., Toimela, T. A., Helenius, M. A. & Kulomaa, M. S. (1994). *Eur. J. Biochem.* **220**, 615–621.
Korkhin, Y., Kalb, A. J., Peretz, M., Bogin, O., Burstein, Y. & Frolow, F. (1999). *Protein Sci.* **8**, 1241–1249.
Korndorfer, I. P. & Skerra, A. (2002). *Protein Sci.* **11**, 883–893.
Kumar, S. & Nussinov, R. (1999). *J. Mol. Biol.* **293**, 1241–1255.
Kumar, S. & Nussinov, R. (2001). *Cell. Mol. Life Sci.* **58**, 1216–1233.
Kurzban, G. P., Bayer, E. A., Wilchek, M. & Horowitz, P. M. (1991). *J. Biol. Chem.* **266**, 14470–14477.
Laitinen, O. H., Airenne, K. J., Marttila, A. T., Kulik, T., Porkka, E., Bayer, E. A., Wilchek, M. & Kulomaa, M. S. (1999). *FEBS Lett.* **461**, 52–58.
Laitinen, O. H., Hytönen, V. P., Ahlroth, M. K., Pentikainen, O. T., Gallagher, C., Nordlund, H. R., Ovod, V., Marttila, A. T., Porkka,

E., Heino, S., Johnson, M. S., Airenne, K. J. & Kulomaa, M. S. (2002). *Biochem. J.* **363**, 609–617.
Laitinen, O. H., Marttila, A. T., Airenne, K. J., Kulik, T., Livnah, O., Bayer, E. A., Wilchek, M. & Kulomaa, M. S. (2001). *J. Biol. Chem.* **276**, 8219–8224.
Lamzin, V. S. & Wilson, K. S. (1993). *Acta Cryst.* D**49**, 129–149.
Livnah, O., Bayer, E. A., Wilchek, M. & Sussman, J. L. (1993). *Proc. Natl Acad. Sci. USA*, **90**, 5076–5080.
Matthews, B. W., Weaver, L. H. & Kester, W. R. (1974). *J. Biol. Chem.* **249**, 8030–8044.
Murshudov, G. N., Vagin, A. A. & Dodson, E. J. (1997). *Acta Cryst.* D**53**, 240–255.
Navaza, J. (1994). *Acta Cryst.* A**50**, 157–163.
Otwinowski, Z. & Minor, W. (1997). *Methods Enzymol.* **276**, 307–326.
Park, S. Y., Yamane, K., Adachi, S., Shiro, Y., Weiss, K. E., Maves, S. A. & Sligar, S. G. (2002). *J. Inorg. Biochem.* **91**, 491–501.
Pazy, Y., Kulik, T., Bayer, E. A., Wilchek, M. & Livnah, O. (2002). *J. Biol. Chem.* **277**, 30892–30900.
Pazy, Y., Raboy, B., Matto, M., Bayer, E. A., Wilchek, M. & Livnah, O. (2003). *J. Biol. Chem.* **278**, 7131–7134.
Perutz, M. F. & Raidt, H. (1975). *Nature (London)*, **255**, 256–259.
Potterton, E., Briggs, P., Turkenburg, M. & Dodson, E. (2003). *Acta Cryst.* D**59**, 1131–1137.
Russell, R. J., Ferguson, J. M., Hough, D. W., Danson, M. J. & Taylor, G. L. (1997). *Biochemistry*, **36**, 9983–9994.
Sano, T., Vajda, S., Smith, C. L. & Cantor, C. R. (1997). *Proc. Natl Acad. Sci. USA*, **94**, 6153–6158.
Scandurra, R., Consalvi, V., Chiaraluce, R., Politi, L. & Engel, P. C. (1998). *Biochimie*, **80**, 933–941.
Vetriani, C., Maeder, D. L., Tolliday, N., Yip, K. S., Stillman, T. J., Britton, K. L., Rice, D. W., Klump, H. H. & Robb, F. T. (1998). *Proc. Natl Acad. Sci. USA*, **95**, 12300–12305.
Vieille, C. & Zeikus, G. J. (2001). *Microbiol. Mol. Biol. Rev.* **65**, 1–43.
Waner, M. J., Navrotskaya, I., Bain, A., Oldham, E. D. & Mascotti, D. P. (2004). *Biophys. J.* **87**, 2701–2713.
Weber, P. C., Ohlendorf, D. H., Wendoloski, J. J. & Salemme, F. R. (1989). *Science*, **243**, 85–88.
Wilchek, M. & Bayer, E. A. (1990). *Methods Enzymol.* **184**, 5–13.
Yip, K. S., Britton, K. L., Stillman, T. J., Lebbink, J., de Vos, W. M., Robb, F. T., Vetriani, C., Maeder, D. & Rice, D. W. (1998). *Eur. J. Biochem.* **255**, 336–346.
Zuber, H. (1988). *Biophys. Chem.* **29**, 171–179.